1990

Determination of Crystallinity and Morphology of Fibrous and Bulk Poly(ethylene terephthalate) by Near-Infrared Diffuse Reflectance Spectroscopy

Charles E. Miller
Haverford College

B. E. Eichinger

9. G. A. Meyer, Anal. Chem. **59**, 1345A (1987).
10. R. F. Browner and A. W. Boorn, Anal. Chem. **56**, 786A (1984).
11. M. Thompson, B. Pahlavanpour, S. J. Walton, and G. F. Kirkbright, Analyst **103**, 568 (1978).
12. M. Thompson, B. Pahlavanpour, S. J. Walton, and G. F. Kirkbright, Analyst **103**, 705 (1978).
13. M. Thompson and B. Pahlavanpour, Anal. Chim. Acta **109**, 251 (1979).
14. R. C. Fry, M. B. Denton, D. L. Windsor, and S. J. Northway, Appl. Spectrosc. **33**, 399 (1979).
15. J. D. Hwang, G. D. Guenther, and J. P. Diomiguardi, Anal. Chem. **61**, 285 (1989).
16. T. Nakahara, Ana. Chim. Acta **131**, 73 (1981).
17. A. Brzezinska-Paudyn, J. Van Loon, and R. Hancock, Atomic Spectrosc. **7**, 72 (1986).
18. R. Bye, Talanta **29**, 797 (1982).
19. D. Nygaard, A. Grindle, and J. Sotera, ICP Inf. Newsl. **14**, 187 (1988).
20. P. D. Goulden, D. H. J. Anthony, and K. D. Austen, Anal. Chem. **53**, 2027 (1981).
21. J. A. C. Broekaert and F. Leis, Fresenius Z. Anal. Chem. **22**, 300 (1980).

Determination of Crystallinity and Morphology of Fibrous and Bulk Poly(ethylene terephthalate) by Near-Infrared Diffuse Reflectance Spectroscopy

CHARLES E. MILLER and B. E. EICHINGER*

Center for Process Analytical Chemistry, Department of Chemistry, BG-10, University of Washington, Seattle, Washington, 98195

Diffuse reflectance spectroscopy in the near-infrared (NIR) region (1100-2400 nm) was used to characterize the morphology of fibrous and bulk poly(ethylene terephthalate) (PET). The method of Partial Least-Squares (PLS) was used to correlate NIR spectra of PET yarns with percent crystallinity. Standard error of prediction values for percent crystallinity in PET yarns are in the range of 2-3.5% crystallinity, and depended on the specific NIR spectral region used for analysis. Principal Components Analysis (PCA) was used to study the differences in NIR spectra of bulk PET samples that were crystallized at different temperatures. It was observed that NIR spectroscopy can detect changes in both intermolecular and intramolecular interactions in PET. The observed effect of crystallization temperature on the morphology of bulk PET is very similar to effects observed in earlier IR and thermal analyses. In addition, detection of moisture in bulk PET is demonstrated.

Index Headings: **Analysis for polymers; Near-infrared spectroscopy; Spectroscopic techniques.**

INTRODUCTION

Poly(ethylene terephthalate) (PET) is currently being used for a wide range of applications. Blow-molded PET is used for food and beverage containers, and drawn PET fibers are used for tire reinforcement.[1] The physical properties of PET depend on several structural factors, such as percent crystallinity, crystallite dimension, and orientation.[2] These structural factors can be influenced by various treatments, such as annealing or drawing, to provide a product with properties appropriate for a specific application. As a result, it is important to determine the effects of these treatments on the structure in order to determine the physical properties of the polymer.

Many different analytical methods have been used to determine structural factors in PET. Infrared and Raman spectroscopy have been used to determine orientation, percent crystallinity, and chain folding at crystalline-amorphous interfaces.[3-12] NMR spectroscopy has been used to characterize the structure of amorphous PET.[13] Wide-angle x-ray scattering (WAXS) can be used to determine percent crystallinity and structure of crystalline domains,[4,14,15] and small-angle x-ray scattering (SAXS) is useful for the determination of crystallite dimensions and orientation of amorphous polymer chains.[14,16,17] The orientation of polymer chains in PET fibers can be determined from birefringence measurements,[2,12,13,18] and differential scanning calorimetry (DSC) yields the percent crystallinity and the presence of different phases in the polymer.[14,18-22]

These methods can provide important structural information about PET. However, they often require extensive sample preparation and long analysis times. As a result, they might not be useful for rapid process analysis. For situations where a rapid analysis is desired, near-infrared (NIR) spectroscopy is very effective.[23-25] The linearity of NIR absorptions and sensitivity of commercial NIR spectrometers allow rapid accurate analyses of relatively unprepared samples, such as wheat[23,26] and bulk polymers.[24,27]

NIR spectra contain bands from overtones and combinations of fundamental vibrational modes. As a result, much of the information present in IR spectra is present in NIR spectra. However, because NIR peaks are considerably broader than IR peaks, absorbances of individual analytes are commonly overlapped. Fortunately, this difficulty can be reduced by the use of multivariate calibration techniques, like Partial Least Squares (PLS)[28-30] and Principal Components Analysis (PCA).[31] These methods can use all spectral frequencies to establish a correlation between NIR spectra and structural features for PET.

The PLS method can calibrate NIR spectra of PET

Received 9 August 1989.
* Author to whom correspondence should be sent.

0003-7028/90/4403-0496$2.00/0

to a specific property, such as percent crystallinity. The ability of NIR spectroscopy to determine the property of interest is indicated by PLS calibration and prediction error statistics. In addition, the PLS regression coefficient spectrum can be used to identify the NIR absorbances, and thus the functional groups, that are affected by the property of interest.

Unlike the PLS method, the PCA method does not determine a specific relationship between NIR spectra and a specific property, but determines the principal component of variation in the NIR spectra of samples with varying properties. The principal components of variation in the NIR spectra correspond to structural variations in the polymer samples. As a result, the scores and loadings spectra obtained from PCA can be used to investigate the structural variations of the different samples. The PCA scores indicate the relationship between the different PET samples used in the analysis, and the PCA loadings spectra indicate the specific NIR spectral features that correspond to the structural variations.

Because the principal components of variation must be orthogonal, they usually do not correspond directly to structural variations in the polymer. Instead, the principal components contain contributions from several structural variations. However, supplementary information about the PET samples, implied from earlier analyses, can be used to assign principal components to specific structural variations.

In this work, the ability of NIR spectroscopy to determine crystallinity and other structural factors in PET is demonstrated. The method of PLS is used to correlate NIR spectra to percent crystallinity in fibrous PET. In addition, PCA analysis of bulk PET crystallized at different temperatures is used to demonstrate the sensitivity of NIR spectroscopy to both crystal growth and crystal perfection mechanisms. Finally, the ability of NIR spectroscopy to distinguish between orientation and crystallinity in PET is demonstrated by PCA analysis of bulk and fibrous PET spectra.

EXPERIMENTAL

Materials. Bulk PET (M_n = 18,000) was obtained from the Goodyear Tire and Rubber Company. Although the exact crystallinity of the bulk PET was unknown, it was assumed that it was mostly amorphous. The pellets were then ground to produce particles in the 500–1000 μm range. Eight 5-g portions of the bulk PET were taken; seven of these were heat-treated at seven different temperatures (110–230°C in 20°C increments) for 5 min in an oil bath with a dry air purge. After heat-treatment, each sample was placed in a vial and allowed to cool to room temperature.

Five different PET tire yarns were also obtained from the Goodyear Tire and Rubber Company. A spun yarn, a fully-drawn yarn, and three underdrawn yarns (10, 20, and 30% underdrawn) were obtained, with the use of the procedure outlined in Ref. 32. X-ray diffraction analyses of the yarns were performed with a Rigaku D-max x-ray spectrometer. The scattering curve for the spun yarn (used as an amorphous reference) was fitted to the diffraction patterns of the other yarns to determine the amorphous fraction of polymer in each, and the remainder of the diffraction pattern for each sample indicated the amount of crystalline polymer. The percent crystallinity values for the PET tire yarns are shown in Table I. The estimated error of the x-ray-determined crystallinity values is 2–3% crystallinity.

TABLE I. Percent crystallinity of PET tire yarns determined by x-ray diffraction.

Sample type	Sample code	Percent crystallinity[a]
Spun	Y0	0
30% Underdrawn	Y1	37
20% Underdrawn	Y2	42
10% Underdrawn	Y3	44
Fully drawn	Y4	42

[a] Estimated error of 2–3% crystallinity.

Spectroscopy. NIR diffuse reflectance spectra of PET powders and yarns were obtained with a Pacific Scientific 6250 NIR grating spectrometer. The spectral range was 1100–2400 nm, the wavelength accuracy was ±1 nm, and the bandpass was 10 nm. Bulk samples were packed into a reflectance sample cup with a quartz window, which was then placed in the spectrometer for NIR analysis. Yarn samples were rolled into a ball and placed into a reflectance sample cup for NIR analysis. Each scan lasted about 30 s. Four scans for each bulk and yarn sample were taken with the sample packed twice in the cell and scanned in two different orientations in the spectrometer.

A near-infrared transmission spectrum of ethylene glycol (EG) (Aldrich) in a 1-mm-pathlength cell and a diffuse reflectance spectrum of terephthalic acid (TPA) (Goodyear Tire and Rubber Co.) in a reflectance sampling cup were used to assist band assignments of PET spectra.

Data Analysis. Before multivariate analysis, each spectrum was corrected for multiplicative and baseline scattering effects by the method of Multiplicative Scatter Correction (MSC).[33] In some cases, the second derivatives of the spectra were taken before MSC correction. The spectra were then split into five different spectral regions for multivariate analysis: I (1100–1350 nm); II (1570–1850 nm); III (1850–2000 nm); and IV (2000–2400 nm).

Principal components analysis was performed for each spectral region with the use of two different data sets: (**A**) bulk PET spectra only, and (**B**) bulk and fibrous PET spectra. Mean-centered spectra were used for all analyses. For each PCA analysis, the number of factors present in the NIR spectra was determined by cross-validation.[31]

PLS calibrations of the yarn spectra to percent crystallinity were constructed with a program provided by the Center for Process Analytical Chemistry.[34] The method of cross-validation was used to determine the optimal number of PLS factors for each calibration. Accuracy of PLS calibrations was expressed according to the Standard Error of Estimate (SEE) value:

$$\mathrm{SEE} = \sqrt{\frac{\sum_{i=1}^{NC} (\hat{C}_i - C_i)^2}{NC - 1}} \qquad (1)$$

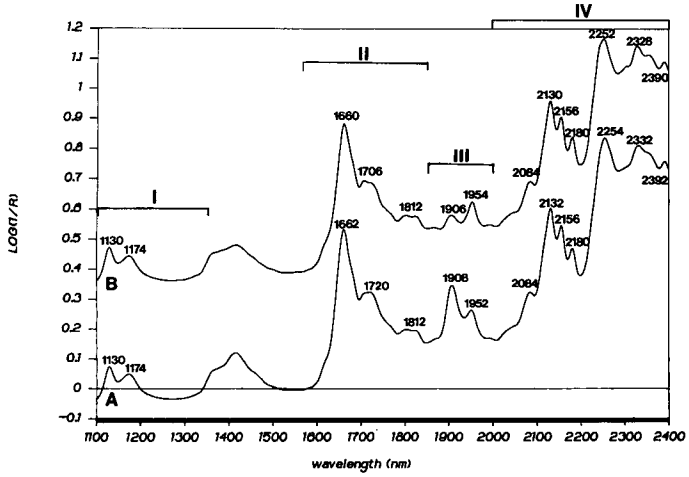

FIG. 1. NIR diffuse reflectance spectra of bulk PET uncrystallized (**A**), and crystallized at 230°C for 5 min (**B**). Specific NIR spectral regions used for analysis are labeled.

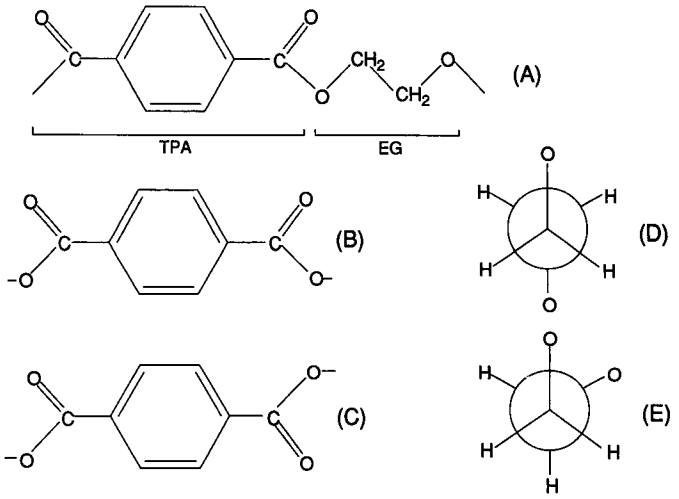

FIG. 2. Chemical structure of the repeat unit in PET (**A**), and various conformational states: planar *cis* configuration of the TPA part (**B**), planar *trans* configuration of the TPA part (**C**), *trans* conformer of the EG part (**D**), *gauche* conformer of the EG part (**E**).

where C_i is the known percent crystallinity of sample i, $\hat{C}_i$ is the percent crystallinity of sample i predicted by the PLS calibration, and NC is the number of calibration samples. Prediction ability of PLS calibrations were expressed according to cross-validated Standard Error of Prediction (SEP) values:

$$\text{SEP} = \sqrt{\frac{\sum_{i=1}^{NP} (\hat{C}_{i,p} - C_i)^2}{NP}}$$

where $\hat{C}_{i,p}$ is the percent crystallinity of sample i predicted by a PLS calibration that does not include sample i, and NP is the number of prediction samples. Only samples Y1, Y2, and Y4, which had intermediate crystallinity values (Table I), were used as prediction samples to determine cross-validated SEP values.

RESULTS AND DISCUSSION

Discussion of PET Spectrum. The NIR diffuse reflectance spectra of bulk PET before and after crystallization at 230°C for 5 min are shown in Fig. 1. The different spectral regions used for analysis are labeled. As one moves from region I to region IV, the absorptivities of the bands increase and the spectral resolution improves. The strong absorbances in region IV have the best spectral resolution, but are highly susceptible to nonlinear behavior. As a result, this region might not provide accurate quantitative results for highly absorbing (or low-scattering) samples.

The chemical structure of PET is shown in Fig. 2A. All of the NIR absorbances are overtone and combination bands of the stretching modes of aromatic C-H groups, methylene groups, and carbonyl groups in the polymer. Regions I, II, and IV contain second-overtone, first-overtone, and combination bands from aromatic C-H groups in the terephthalic acid (TPA) part and methylene groups in the ethylene glycol (EG) part. Region III contains the second-overtone carbonyl stretching band and absorbances from moisture in the polymer.

Specific assignments of NIR bands are difficult to determine, because the absorptions from each vibrational overtone and combination are highly overlapped. However, approximate assignments can be made from previously assigned bands in the IR and Raman spectra of PET[3,6–8,11] and from NIR spectra of ethylene glycol and terephthalic acid. Frequencies of NIR overtone bands are approximately integer multiples of IR fundamental frequencies, and frequencies of NIR combination bands are approximately the summation of IR fundamental frequencies of the modes contributing to the combination. The assignments of NIR bands in the PET spectra are listed in Table II. It should be mentioned that the 2254-nm methylene combination band for PET is at a significantly higher frequency than the methylene combination band for ethylene glycol (2285 nm). The cause of this difference is probably the larger electron withdrawing effect of neighboring carboxyl groups in PET relative to neighboring hydroxyl groups in ethylene glycol.

Although the spectroscopic differences between uncrystallized and crystallized PET in the NIR region (Fig. 1) are not as dramatic as in the IR region,[3,6–8,11] significant differences are observed. In region IV, the ethylene combination bands at 2254 and 2332 nm (Fig. 1A) each shift to higher frequency (lower wavelength) with crystallization. Because the methylene bending and wagging vibrations are each higher for the *trans* conformer than for the *gauche* conformer of the EG segment and because the methylene stretching frequency is relatively unaffected by crystallization,[3] the positive energy shifts of these combination bands are a result of an increase in the *trans/gauche* conformer ratio with crystallization. It should also be noted that the spectrum of the crystallized sample (Fig. 1B) has more fine structure than the spectrum of the uncrystallized sample (Fig. 1A) in the region from 2300 to 2400 nm. This discrepancy is probably caused by crystal field splitting of bands in this region.

The bands in region II, which are primarily first-overtone C-H aromatic and methylene stretching bands, also change upon crystallization. These differences might be a result of differences in inter- or intramolecular order

TABLE II. Positions and assignments for peak maxima in spectra of PET and model compounds.

Spectral region	Band maxima (nm) PET NC[a]	PET C(230C)[b]	Models TPA[c]	Models EG[d]	Band assignment
I	1130	1130	1126	···	2nd overtone aromatic C-H stretch
I	1174	1174	···	1206	2nd overtone methylene stretch
II	1662	1660	1656	···	1st overtone aromatic C-H stretch overlapped with 1st overtone methylene stretch
II	1720	1706	···	1713	1st overtone methylene stretch
II	1812	1812	···	···	(3rd overtone methylene bend)
III	1908	1906	···	···	O-H stretch and bend combination, water (Ref. 23)
III	1952	1954	···	···	2nd overtone C=O stretch (Ref. 23)
IV	2084	2084	2090	···	3rd overtone C-O stretch (Ref. 23)
IV	2132	2130	2131	···	Combination aromatic C-H stretch and ring vibration
IV	2156	2156	2155	···	Combination aromatic C-H stretch and ring vibration
IV	2180	2180	2180	···	Combination aromatic C-H stretch and ring vibration
IV	2254	2252	···	2285	Combination methylene stretch and bend
IV	2332	2328	2332	···	Overlap of absorbances involving methylene and aromatic C-H groups and COO groups
IV	2392	2390	···	···	

[a] NC = uncrystallized bulk PET.
[b] C(230C) = bulk PET crystallized at 230°C for 5 min.
[c] Terephthalic acid.
[d] Ethylene glycol.

for the two samples. Intermolecular order is characterized by the ordered chain packing present in crystalline material, and intramolecular order depends on the conformational structure of individual chains. The weaker and broader second-overtone C-H stretching bands in region I do not appear to change with crystallization. However, more detailed multivariate analyses can detect small spectral shifts in this region and in other regions.

In region III, a large decrease in the 1908-nm water band with crystallization is observed. This result indicates that moisture originally present in the polymer was removed during annealing at 230°C. A more detailed discussion of this effect will be presented later.

PLS: Crystallinity in Yarns. The results of PLS calibrations for crystallinity in PET fibers are shown in Table III. A successful crystallinity determination for PET yarns requires the ability to distinguish between crystalline polymer, oriented amorphous polymer, and random amorphous polymer. Crystalline domains are characterized by specific intermolecular and intramolecular order, whereas oriented amorphous PET is characterized by intramolecular order. In spectroscopic terms, the vibrations of methylene and aromatic C-H and carbonyl groups in the polymer (and therefore the spectrum of the polymer) must be sensitive not only to intramolecular order but also to intermolecular interactions.

The PLS cross-validation results, which indicate the number of independent spectral factors present in the NIR spectra of the PET yarns, are shown in the last column of Table III. For spectral regions I, II, and IV, the PLS calibration required the use of two factors. Therefore, one can assume the presence of two independent spectral variations in the PET yarn spectra. It is quite possible that these two independent variations correspond to changes in intermolecular and intramolecular states in the polymer. It is therefore possible that the NIR spectra in these regions contain enough information to allow one to determine percent crystallinity in the yarns.

For the most part, the use of second-derivative spectra improves PLS prediction results. This improvement is caused by removal of baseline variations and enhancement of spectral resolution. NIR spectral regions II and IV provide the best results for crystallinity determinations. Because the combination bands in region IV are

TABLE III. Results of PLS calibrations for percent crystallinity in PET yarns.

Spectral region	Spectral correction	Calibration statistics (in % crystallinity) Calibration SEE	Prediction SEP	Number of factors[a]
I	None	4.44	5.84	2
I	Second deriv.[b]	2.54	3.68	2
II	None	1.88	3.51	2
II	Second deriv.	1.05	2.76	2
III	None	3.89	5.43	1
III	Second deriv.	2.89	3.98	1
IV	None	1.87	2.72	2
IV	Second deriv.	1.37	2.11	2

[a] Determined by cross-validation.
[b] Second derivative.

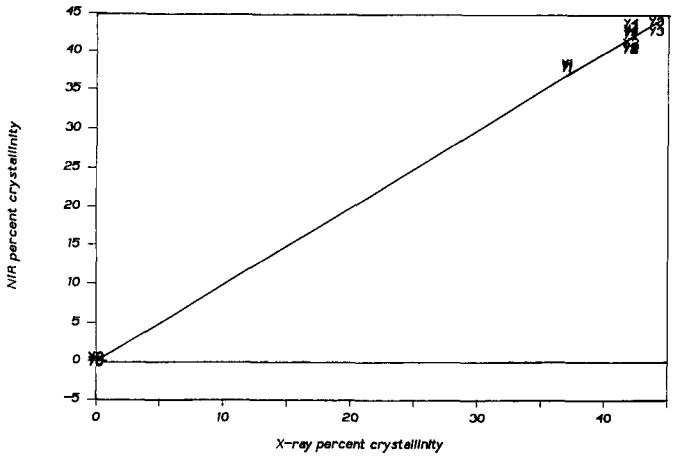

FIG. 3. PLS calibration curve for percent crystallinity in PET yarns. Second-derivative spectra in region II are used for the calibration. Sample labels are listed in Table I.

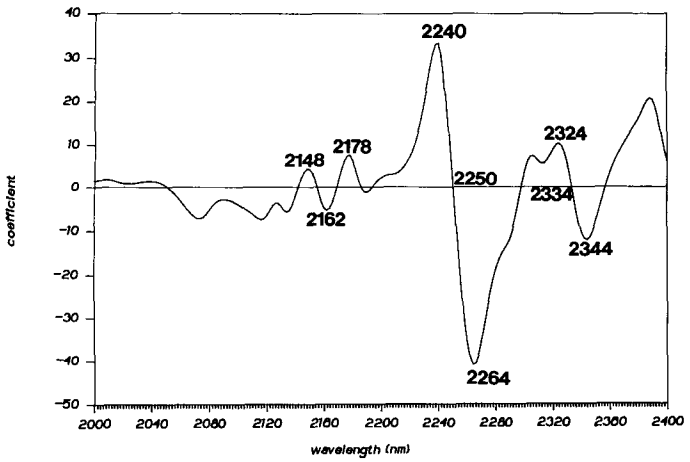

FIG. 4. PLS regression coefficient spectrum for the percent crystallinity calibration that uses normal spectra in region IV.

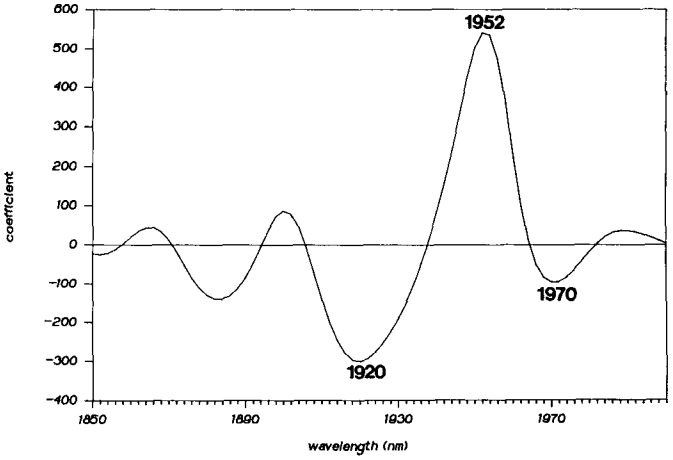

FIG. 5. PLS regression coefficient spectrum for the percent crystallinity calibration that uses normal spectra in region III.

better resolved than the overtone bands in region II, the prediction results for region IV are the most favorable. However, the weaker absorbances in region II are less likely to be nonlinear as a result of stray light effects. Therefore, region II might provide the best results for highly absorbing (low-scattering) samples. The prediction results for region I are less favorable, because the absorptions are weak and highly overlapped. However, this region might be optimal for analysis of thick (1–2 cm) PET films, which would produce stronger absorbances in this region and nonlinear absorbances in the other regions.

It should be mentioned that the calibration and prediction errors for the calibrations that use regions II and IV are close to the estimated error of the x-ray crystallinity values (2–3% crystallinity). This result suggests that the error in the x-ray crystallinity values is the limiting error for these calibrations. As a result, better calibrations might be possible if a more accurate reference crystallinity measurement is used.

The calibration curve for the PLS calibration that uses second-derivative spectra in region II is shown in Fig. 3. Although five different yarn samples are used to construct the calibration, there are essentially three different crystallinities represented in the calibration, because differences in the crystallinities of the fully-drawn, 10% underdrawn, and 20% underdrawn samples are within the error of the x-ray crystallinity measurement. Furthermore, these crystallinity values are not well distributed over the range of crystallinities. Therefore, it could be argued that a poor design of the calibration samples, which is not intentional but is dependent on the yarn samples that are available, results in overfitting of the calibrations. However, the cross-validation results, which indicate the maximum number of PLS factors that can be used to avoid overfitting, are very reliable. As a result, it is probable that overfitting did not occur in the PLS calibrations, despite the relatively poor design of the calibration samples.

The regression coefficient spectrum for the PLS calibration that uses normal spectra in region IV is shown in Fig. 4. The first-derivative features at 2250 and 2334 nm indicate negative wavelength shifts (positive frequency shifts) of the methylene combination bands with crystallization. As mentioned earlier, these shifts indicate an increase in the *trans/gauche* conformer ratio with increasing crystallinity. This result is expected, because only the *trans* conformer is present in crystalline PET.[15] The weaker features at 2148, 2162, and 2178 nm indicate shifts or sharpening of aromatic C-H combination bands with crystallinity. These features are probably a result of the increased intermolecular order associated with crystalline material.

Only one PLS factor was necessary for each calibration that used spectral region III. Therefore, it is doubtful that this region provides enough information to accurately determine crystallinity in PET yarns. Prediction errors are significantly greater for this spectral region than for regions II and IV, which have comparable absorbance intensities and spectral resolution. However, region III contains enough information to provide an approximate crystallinity determination.

The PLS regression coefficient spectrum for the calibration that uses region III is shown in Fig. 5. A positive peak at 1952 nm is flanked by two negative side lobes at 1920 and 1970 nm. This feature suggests that an increase in crystallinity is accompanied by a slight narrowing of the carbonyl band at 1952 nm. This result is in agreement with results from earlier Raman analyses of PET,[6] which indicated that the half-width of the fundamental carbonyl stretching band decreases with increasing crystallinity.

PCA of PET Powder Spectra. The PCA cross-validation results for the NIR spectra of bulk PET crystallized at different temperatures (data set **A**) are shown in Table IV. These results indicate that there are two independent spectral trends with crystallization temperature for regions I, II, and IV. The presence of two independent spectral variations in the NIR spectra indicates that two independent structural variations of PET polymer chains occur as a function of annealing temperature.

Detailed theoretical[35] and experimental[36,37] work on polymer crystallization has provided information about structural changes that occur with crystallization. In general, structural changes result from crystal growth and crystal perfection mechanisms. Crystal growth involves the aggregation of previously amorphous polymer chains into crystalline domains. This process is characterized

TABLE IV. Number of factors for PCA analyses, determined by cross-validation.

Data set A: Spectra of bulk PET crystallized at different temperatures.

Spectral region	Spectral correction	Number of factors used
I	None	3
I	Second derivative	2
II	None	2
II	Second derivative	2
III	None	1
III	Second derivative	1
IV	None	2
IV	Second derivative	2

Data set B: Spectra of bulk PET crystallized at different temperatures and spectra of PET yarns spun and drawn to different extensions.

Spectral region	Spectral correction	Number of factors used
I	None	2
I	Second derivative	2
II	None	2
II	Second derivative	2
III	None	1
III	Second derivative	1
IV	None	2
IV	Second derivative	2

by an increase in intramolecular and intermolecular order. Crystal perfection involves rearrangements of polymer chains that eliminate defects in the crystalline domains. These rearrangements might involve the formation of chain folds at the surface of crystalline domains, diffusion of internal defects from the crystalline domains, or elimination of the tie chains that span different crystalline domains. Earlier results of thermal analysis of PET[19,20] suggested that crystal growth occurs at 100–245°C, but substantial rearrangements and crystal thickening can occur only at crystallization temperatures above 200°C.

Both crystal growth and perfection involve major structural changes that should be detectable by vibrational spectroscopy. Indeed, IR analyses[10] of crystallized PET indicated the presence of two distinct spectral trends with crystallization temperature. It was suggested that a crystal growth process can occur at annealing temperatures below 160°C, and a rearrangement process occurs at crystallization temperatures above 160°C. As expected, the crystal growth mechanism involved an increase in the *trans/gauche* conformer ratio. In contrast, the rearrangement mechanism involved a decrease in the *trans/gauche* ratio for the amorphous phase.

The PCA scores and loading spectra for the analysis that uses spectral region IV are shown in Figs. 6 and 7, respectively. Despite the scatter between replicate samples in the PCA scores plot (Fig. 6), a distinct nonlinear spectral trend with crystallization temperature is indicated. For low crystallization temperatures (samples B0 to B4), a fairly linear decrease in the first principal component with crystallization temperature is observed. A curve in the trend occurs at samples B4 and B5, which are crystallized at 170 and 190°C. The samples crystallized at higher temperatures (B6 and B7) follow a different trend, which is a decrease in the second principal

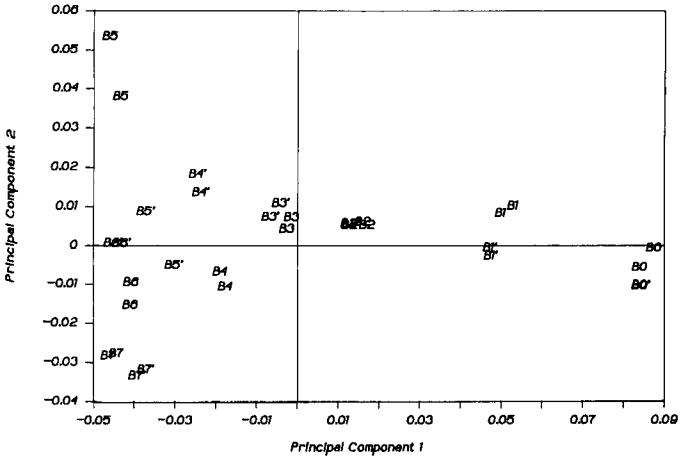

FIG. 6. Scores plot from the principal components analysis of spectra (in region IV) of bulk PET samples crystallized for 5 min at different temperatures. Crystallization temperatures corresponding to different labels are as follows: B0, uncrystallized sample; B1, 110°C; B2, 130°C; B3, 150°C; B4, 170°C; B5, 190°C; B6, 210°C; B7, 230°C. Primes on sample labels denote repacked samples.

component with crystallization temperature. As a result, the scores plot indicates that two different spectral trends with crystallization temperature occur: one that dominates for crystallization temperatures below 170–190°C, and one that dominates for higher crystallization temperatures. This result is in agreement with IR and thermal analyses of PET.[10,19,20] To a first approximation, the first principal component (x-axis) is inversely related to the low crystallization temperature trend (affecting samples B0 to B5), and the second principal component (y-axis) is inversely related to the high crystallization temperature trend (which affects samples B6 and B7).

The loading spectra for the first two principal components are shown in Fig. 7. The most prominent features in the first principal component loading spectrum are first-derivative features at 2256 and 2332 nm, where the strong ethylene combination bands (Table II) are situated. These derivative features indicate negative energy band shifts with increasing principal component score 1, which correspond to positive energy shifts of these bands

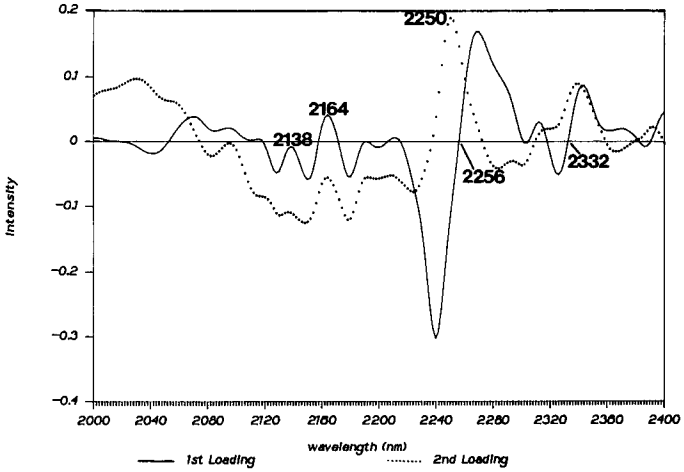

FIG. 7. Loadings spectra from the principal components analysis of spectra (in region IV) of bulk PET crystallized for 5 min at different temperatures. Solid line, first principal component loading; dotted line, second principal component loading.

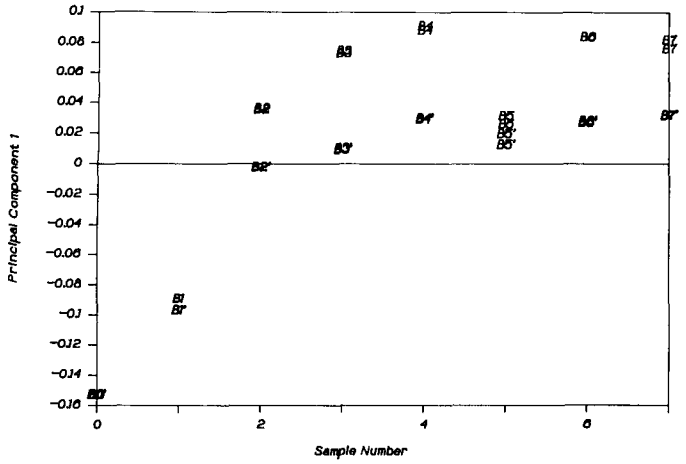

FIG. 8. Plot of the first principal component score vs. sample number from the principal components analysis of spectra (in region III) of bulk PET crystallized for 5 min at different temperatures. Sample labels are identical to those used in Fig. 6.

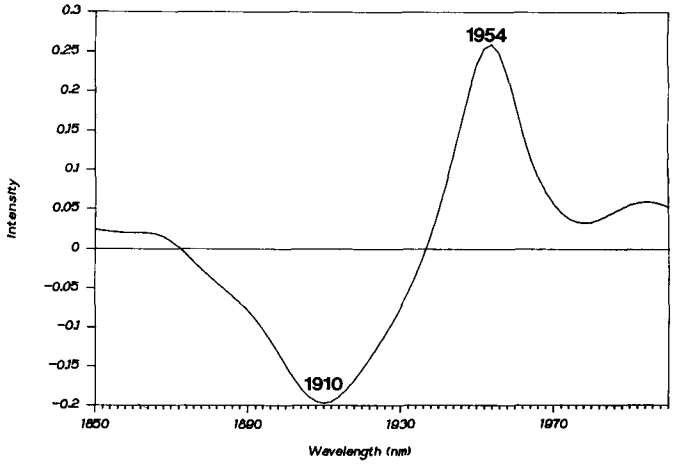

FIG. 9. Loadings spectrum from the principal components analysis of spectra (in region III) of bulk PET crystallized for 5 min at different temperatures.

with crystallization temperature for low crystallization temperatures. This result indicates that the low crystallization temperature trend corresponds to an increase in the *trans/gauche* conformer ratio with crystallization temperature. As a result, the NIR spectral data support a crystal growth mechanism for the low crystallization temperature trend.

The first principal component loading spectrum shows features at 2138 and 2164 nm, where aromatic C-H combination bands are found. These features suggest that aromatic C-H stretching and bending vibrations in the terephthalic acid part of the polymer are affected by crystal growth. Both the planar *cis* and planar *trans* configurations of the carbonyl groups about the aromatic ring in the TPA part (see Fig. 2, B and C) are possible in amorphous material,[38] but only the planar *trans* configuration is observed in crystalline material.[15] Because the aromatic vibrations in a given TPA segment are affected by the configuration of the neighboring carbonyl groups, a change in aromatic C-H combination absorbances with percent crystallinity is expected. In addition, the increase in intermolecular order associated with crystalline material probably perturbs the aromatic vibrations.

The structural origin of the high crystallization temperature trend is indicated by the second principal component loading spectrum (in Fig. 7). The most distinguishing feature of the second principal component loading spectrum is the positive band at 2250 nm. Because this band is located at the high-frequency side of the ethylene combination band in PET (Table II), it indicates an increase in the *trans* conformer in the ethylene glycol unit with increasing principal component score 2. This result translates to a decrease in the *trans/gauche* ratio with crystallization temperature. This result is in agreement with results of earlier IR analyses of crystallized PET, in which the *trans* conformer content in the amorphous phase was found to decrease at crystallization temperatures above 170°C.[8]

There are several aspects of crystal perfection that could explain the observed high crystallization temperature trend. Earlier, it was proposed that depletion of tie chains (which are polymer chains that connect crystalline domains) occurs at high crystallization temperatures.[8] It was also concluded that, because these tie chains contain a disproportionately large fraction of *trans* conformers in the amorphous phase, loss of them would result in a decrease in the total number of *trans* conformers. The decrease in tenacity of PET fibers annealed at high temperatures supports this explanation, because tenacity of PET fibers is directly related to the number of tie chains.[2]

If loss of tie chains occurs at high crystallization temperatures, a gain in other structural features (which contain more *gauche* conformers) must also occur. Sharpening of the phase boundaries between crystalline and amorphous material might cause an increase in the *gauche* conformer content. The sharpening of a phase boundary corresponds to the narrowing of the interfacial region between amorphous and crystalline polymer, and requires an increase in the number of polymer chains that escape and re-enter the same crystallite.[39] In order for a chain to escape and re-enter the same crystallite, a turn or fold of the chain must be present. Because a chain fold must contain more *gauche* conformers than *trans* conformers, it is expected that an increase in chain folding (corresponding to a sharpening of phase boundaries) would cause an overall increase in the number of *gauche* conformers.

Moisture Effect. The principal component scores for the analysis that uses normal spectra in region III are shown in Fig. 8. The uncrystallized samples and the samples crystallized at 110°C (samples B0 and B1) fall into tightly bound clusters. However, the scores for the samples crystallized at 130°C and at higher temperatures indicate a significant repacking effect. For sample B5, which is crystallized at 170°C, the effect is not large. In all other cases, the effect is characterized by a decrease in the first principal component score as a result of repacking the sample. The trend with crystallization temperature, which is obscured by the repack effect, is an increase in the first principal component score.

The first principal component loading spectrum for region III is shown in Fig. 9. The minimum at 1910 nm indicates that the first principal component corresponds

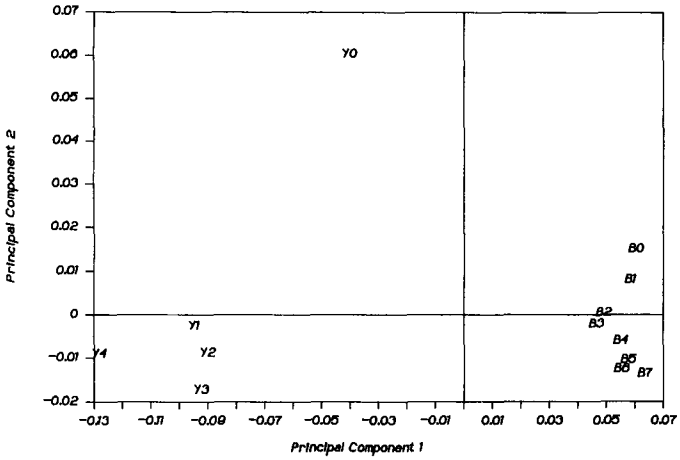

FIG. 10. Plot of the second principal component score vs. the first principal component score, from the principal components analysis of spectra (in region II) of both fibrous PET drawn to different extensions and bulk PET crystallized for 5 min at different temperatures. Sample labels are identical to those used in Fig. 6 and Table I. Average principal component scores values for replicate samples are used for clarity.

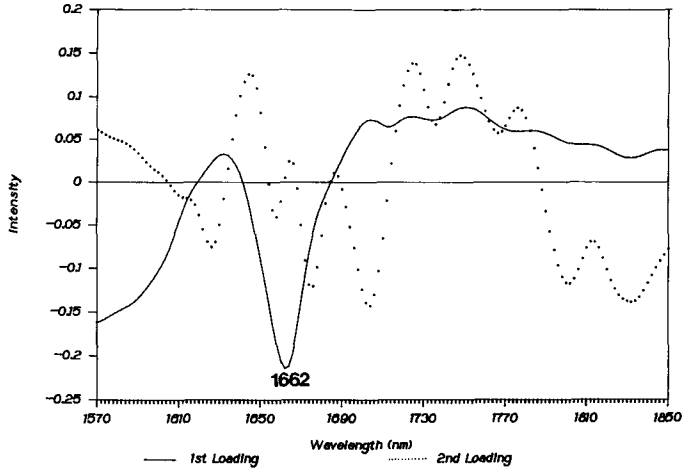

FIG. 11. Loadings spectra from the principal components analysis of spectra (in region II) of both fibrous PET drawn to different extensions and bulk PET crystallized at different temperatures. Solid line, first principal component loading; dotted line, second principal component loading.

to a decrease in the absorbance of the water band. Because the repack effect involves a decrease in the first principal component score, it correlates to an increase in the moisture content. Apparently, moisture originally present in the uncrystallized bulk PET is removed during crystallization at temperatures above 110°C. Subsequent exposure of the samples to the atmosphere before original sampling and during the repack procedure allowed the samples to absorb moisture from the air.

The sample vials used to contain the samples after crystallization and before NIR analysis and the reflectance sampling cup protected the samples from atmospheric moisture. However, the samples were exposed to the atmosphere during the transfer from sampling vial to sampling cup and during the repack procedure. The PCA results indicate that the samples absorb moisture from the atmosphere during the repack procedure. The anomalous behavior of sample B5 (Fig. 8) might be caused by a leaky sample vial, which allowed the sample to absorb a significant amount of atmospheric moisture before NIR analysis.

There are two important implications of the observed moisture effect. The presence of water in the amorphous polymer might cause hydrolysis of the polymer during crystallization.[1] However, the absorptivity of the 1908-nm water band is approximately 25 times the absorptivity of the 1952-nm carbonyl band,[40] and the intensities of these two bands in the spectrum of the amorphous PET (Fig. 1A) are comparable. Therefore, the amount of water in the amorphous polymer is rather small, and it is expected that only a small amount of hydrolysis occurred in the crystallized samples. In addition, regions I, II, and IV are dominated by CH bands, and are therefore insensitive to the small amount of hydrolysis that might occur upon crystallization.

The second implication of the moisture effect is the ability of NIR spectroscopy to determine moisture in PET. The moisture content of the amorphous polymer before processing is a very important control variable in many applications. Water in the pre-processed polymer might cause hydrolysis of the polymer during high-temperature processing, which decreases the average molecular weight and therefore degrades the quality of the processed material.[1]

PCA of Powder and Fiber Spectra. The ability of NIR spectroscopy to discriminate between orientation and crystallinity in PET is demonstrated by principal components analysis of a data set comprised of both fibrous and bulk PET spectra. For analyses that use regions I, II, and IV, the optimal number of PCA factors is two (Table IV). Because the PCA analyses of bulk PET spectra alone also indicated the presence of two factors, it can be concluded that the same spectral trends in these regions used to describe variations in the bulk PET spectra can also be used to distinguish between fibrous and bulk PET spectra.

The scores and loading spectra for PCA analysis of normal spectra in region II are shown in Figs. 10 and 11, respectively. The first principal component score is inversely related to the draw ratio of the yarns, and discriminates between bulk and fibrous PET samples. As a result, the first principal component is inversely related to chain orientation in the polymer. The second principal component score is inversely related to crystallinity of the PET yarns and inversely related to the low crystallization temperature trend for bulk PET samples. These results indicate that the second principal component is inversely related to crystallinity.

Note that the high crystallization temperature trend for the bulk PET samples, which involves samples B6 and B7 (Fig. 10), corresponds to an increase in the first principal component score with increasing crystallization temperature. This result suggests that a structural trend involving decreased orientation can be used to describe the high crystallization temperature trend for crystallized bulk PET. This structural trend is most likely a decrease in the *trans/gauche* conformer ratio, which is consistent with results discussed earlier and with results of past IR analyses of PET.[8]

The principal component loading spectra are shown in Fig. 11. Because the spectral resolution in region II is significantly lower than in region IV, detailed structural

information is difficult to obtain from the loading spectra. However, the two loading spectra show striking differences. The first loading, which describes spectral variation inversely related to orientation, is very featureless. The negative peak at 1662 nm is at the same position as the peak assigned to the first overtone aromatic C-H stretch (Table II), and might indicate a sharpening of this band with increased orientation. However, it is probable that a large overlap of methylene and aromatic C-H absorbances is present in this region. Therefore, it is quite possible that a change in the *trans/gauche* conformer ratio is also indicated in this loading spectrum. The second principal component loading spectrum, which indicates spectral changes inversely related to crystallinity, is very different from the first principal component loading spectrum. This loading spectrum indicates the sharpening or shifting of absorbances in this region, which is indicative of an increase in intramolecular and intermolecular order caused by crystallization.

CONCLUSION

This study has shown that NIR spectroscopy can be used to perform rapid and accurate analyses of fibrous and bulk PET for various processing applications. Results of PLS calibrations for percent crystallinity in PET fibers and PCA analyses of spectra of fibrous and bulk PET indicate that NIR spectroscopy can characterize both intramolecular and intermolecular effects, and thus distinguish between crystallinity and orientation. Although other analytical methods are better suited for detailed structural investigations, this work has shown that NIR spectroscopy is sensitive to the structural features in PET that influence the physical properties and quality of PET products.

ACKNOWLEDGMENTS

The authors would like to thank the Goodyear Tire and Rubber Company for organizing a 1988 summer internship, during which the data were collected. Specific acknowledgments go to Dr. Thomas W. Gurley and James G. Hermiller for helpful guidance and suggestions, Dr. R. N. Thudium, for x-ray crystallinity determinations, Kevin Westgate for the PET yarn samples, and Dr. Ben Duh for bulk PET samples and crystallization work. Comments from Dr. Ed Johnson at the Center for Process Analytical Chemistry were very helpful.

1. Modern Plastics, **64(10A)**, 44 (1987).
2. R. T. Samuels, in *Structured Polymer Properties* (Wiley-Interscience, New York, 1974), p. 211.
3. I. M. Ward, Chem. Ind. (London) **1957**, 905 (1957).
4. G. Farrow and I. M. Ward, Polymer **1**, 330 (1960).
5. P. G. Schmidt, J. Poly. Sci., A, **1**, 1271 (1963).
6. A. J. Melveger, J. Poly. Sci., A-2, **10**, 317 (1972).
7. L. D'Esposito and J. L. Koenig, J. Poly. Sci., Phys. Ed. **14**, 1731 (1976).
8. S.-B. Lin and J. L. Koenig, J. Poly. Sci., Phys. Ed. **20**, 2277 (1982).
9. J. Stokr, B. Schneider, D. Doskocilova, J. Lovy, and P. Sedlacek, Polymer **23**, 714 (1982).
10. S.-B. Lin and J. L. Koenig, J. Poly. Sci., Phys. Ed. **21**, 2365 (1983).
11. L. J. Fina and J. L. Koenig, Macromolecules **17**, 2572 (1984).
12. H. M. Heuvel and R. Huisman, J. Appl. Poly. Sci. **30**, 3069 (1985).
13. H. G. Zachmann, Poly. Eng. and Sci. **19**, 966 (1979).
14. S. Fakirov, E. W. Fischer, R. Hoffmann, and G. F. Schmidt, Polymer **18**, 1121 (1977).
15. R. P. Daubeny, C. W. Bunn, and C. J. Brown, Proc. Roy, Soc. A **226**, 531 (1954).
16. L. H. Palys and P. J. Phillips, J. Poly. Sci., Phys. Ed. **18**, 829 (1980).
17. E. Burnshlegl and R. Bonart, Colloid and Poly. Sci. **258**, 319 (1980).
18. V. B. Gupta and S. Kumar, J. Appl. Poly. Sci. **26**, 1865 (1981).
19. G. Groeninckx, H. Reynaers, H. Berghmans, and G. Smets, J. Poly. Sci., Phys. Ed. **18**, 1311 (1980).
20. G. Groeninckx and H. Reynaers, J. Poly. Sci., Phys. Ed. **18**, 1325 (1980).
21. E. Ito, K. Yamamoto, Y. Kobayashi, and T. Hatakeyama, Polymer **19**, 39 (1978).
22. R. C. Roberts, Polymer **10**, 117 (1969).
23. P. Williams and K. Norris, *Near-Infrared Technology in the Agricultural and Food Industries* (American Association of Cereal Chemists, St. Paul, Minnesota, 1987).
24. L. G. Weyer, Appl. Spectrosc. Rev. **21**, 1 (1985).
25. E. Stark, K. Luchter, and M. Margoshes, Appl. Spectrosc. Rev. **22**, 335 (1986).
26. K. Norris and P. C. Williams, Cereal Foods World **24**, 459 (1979).
27. C. E. Miller, Appl. Spectrosc. **43**, 1435 (1989).
28. K. Beebe and B. R. Kowalski, Anal. Chem. **59**, 1007A (1987).
29. P. Geladi and B. R. Kowalski, Anal. Chim. Acta **185**, 1 (1986).
30. D. M. Haaland and E. V. Thomas, Anal. Chem. **60**, 1202 (1988).
31. I. T. Jolliffe, *Principal Component Analysis* (Springer-Verlag, New York, 1986).
32. D. L. Brown, J. T. Weissert, R. S. Bhakuni, and G. S. Rogowski, U.S. Patent 4,654,253, March 31, 1987.
33. P. Geladi, D. MacDougall, and H. Martens, Appl. Spectrosc. **39**, 491 (1985).
34. D. Veltkamp and B. R. Kowalski, *PLS-2 Block Modeling, Version 1.9* (IBM) (Center for Process Analytical Chemistry, Seattle, Washington, 1987).
35. D. M. Sadler and G. H. Gilmer, Polymer **25**, 1446 (1984).
36. D.-Y. Yoon and P. J. Flory, Faraday Discuss. Chem. Soc. **68**, 288 (1979).
37. E. W. Fischer, Polymer J. **17**, 397 (1985).
38. A. D. Williams and P. J. Flory, J. Poly. Sci., A-2 **5**, 417 (1967).
39. L. Mandelkern, *Crystallization of Polymers* (McGraw-Hill, New York, 1964).
40. R. F. Goddu and D. A. Delker, Anal. Chem. **32**, 140 (1960).